Research on the Dynamics and Evolution of Regional Blue-green Space Driven by the Development of World-class Urban Agglomerations

Ziwu Pan
Henan University
Jun Zhu
Henan University
Zhenzhen Liu
Henan University
Fen Qin (qinfun@126.com)
Henan University

Research Article

Keywords: urbanization, Shanghai, Nanjing and Suzhou, land surface temperature (LST) and regional thermal environment (RTE)

Posted Date: June 22nd, 2021

DOI: https://doi.org/10.21203/rs.3.rs-598367/v1

Research on the dynamics and evolution of regional Blue-green space driven by the development of world-class urban agglomerations

Ziwu Pan[1,2], Jun Zhu[1,2], Zhenzhen Liu[1,2], and Fen Qin[1,2*]

1 College of Environment and Planning, Henan University, Kaifeng, China; wugemicheal@163.com (Z.P.); 419974539@qq.com (J.Z.); 635522875@qq.com(Z.L.).
2 Key Laboratory of Geospatial Technology for the Middle and Lower Yellow River Regions, Henan University, Kaifeng, China
* Correspondence: qinfun@126.com; Tel.: +86-135-0378-5302; Fax: +86-0371-23881850

Abstract: In recent years, the process of urbanization in China has accelerated, and changes in the underlying surface have caused the difference in average temperature between built-up areas and suburbs to increase, resulting in an urban heat island effect, which has become an important environmental issue for today's urban sustainable development. The Yangtze River Delta urban agglomeration region is the fastest-growing region in China, with economically developed and populous cities such as Shanghai, Nanjing and Suzhou. It has become one of the six major urban agglomerations in the world, and its heat island effect is particularly prominent. The single urban heat island phenomenon gradually evolves into the urban agglomeration heat island phenomenon with urbanization. However, the dynamic transfer process of key blue-green space landscapes that can alleviate land surface temperature (LST) and regional thermal environment (RTE) is still poorly understood, especially in the context of urban agglomerations. With the approval of the State Council on the development plan of the Huaihe River Ecological Economic Belt, the construction of which has been officially upgraded to a national strategy. The Eastern HaiJiang River and Lake Linkage Zone (EJRLLZ) emphasizes strengthening the docking and interaction with the surrounding areas such as the Yangtze River Delta and the Wanjiang City Belt. With the diffusion of the heat island effect of the Yangtze River Delta urban agglomeration, as one of the

areas with great potential development around the world-class urban agglomeration, the rich water body and green space in the ERLLZ area are also destroyed and affected. Therefore, we take this region as a case to further quantify the impact of urbanization and urban agglomeration development on the dynamics and evolution of blue-green space.

In this study, MODIS land surface temperature products and Globe land cover products were used for analysis. With the help of Google cloud computing, Markov model and spatial analysis, the seasonal and interannual variations of land surface temperature and relative land surface temperature in the study area from 2000 to 2020 were analyzed from the perspective of temporal and spatial changes.This paper reveals that (1) there are significant differences in the cooling effect of the gains and losses of ecological land, which provides evidence for the value of the existing natural ecological system (especially forest land) to climate adaptation because the newly constructed ecological land does not provide the same cooling effect. (2) Land cover change is not only affected by land cover patterns and processes, but also significantly affected by specific land conversion processes. (3) From 2000 to 2020, the development land in the ERLLZ increased significantly, while the arable land decreased significantly. The urban cooling island was gradually isolated and dispersed, and the urban heat island was interconnected and interacted to form a regional heat island. This study deepens the understanding of the dynamics and evolution of blue-green space in the context of urban agglomerations, and provides an important perspective for the protection of existing natural ecosystems and climate adaptation planning.

Keywords: Rapid urbanization; Land conversion processes; Blue-green space; Regional cooling environment;

1. Introduction

With the advancement of global warming and urbanization, extreme high temperature weather occurs frequently all over the world, which has a serious impact on the health of residents. For example, in mid-July 1995, Chicago suffered a heat wave attack, just a week more than 700 people died of heat stroke. In the summer of 2003, about 35000 people died of heat waves in Europe and 1400 people died of high temperature in India. The second and third national assessments of climate change also indicate that the average rate of surface warming in China is significantly higher than that in other countries or regions of the world over the same period [1-4]。Since the reform and opening up, China's urbanization has been very rapid. In 2011, China's urbanization level has exceeded 50 %, reaching a high level, and it is still in the process of rapid urbanization. Rapid urbanization has significantly changed the urban landscape process and pattern evolution, especially resulting in an increase in the impervious area of urban surface, changing the thermal properties of urban surface, resulting in changes in the atmospheric structure of near-surface strata in urban areas, resulting in ecological environmental consequences such as urban heat island effect. Urban heat island effect is the phenomenon that the temperature in the city is significantly higher than that in the peripheral suburbs, which is the most significant feature of urban climate. Therefore, how to alleviate urban high temperature has become a hot research topic in many disciplines and fields, such as urban thermal environment effect, climate change, urban natural disasters.

Blue and green spaces such as mountains, rivers, lakes, green spaces and wetlands play an important role in regulating and improving local climate and environment. Through the protection, restoration and construction of urban blue and green space system, improving urban internal permeability and microcirculation ability has become an important way for urban spatial planning and design to deal with local climate and environment problems. Many studies claim that the development of urban blue-green space may be a better solution

than cool materials, because urban blue-green space has the characteristics of high cost-effectiveness and environmental friendliness. Urban water, including rivers, lakes and wetlands (reservoirs, ponds), is an important ecological space of the city, commonly known as the 'blue system'. Urban green spaces include mountains, woodlands, farmlands, grasslands, ecological corridors, open spaces such as large green spaces, strip green spaces, protective green spaces, public green spaces and urban green roofs, which are called 'green systems' [5]. In recent years, domestic and foreign scholars have conducted a large number of detailed studies on the blue-green space mitigation of urban heat island effect.

Previous studies have found that the cooling island effect of blue-green space depends on the size, shape, connectivity and complexity (composition and configuration) of blue-green space [6,7]. Zhou et al. found that the cooling effect of park green space on the surrounding area decreased with the increase of distance [8]. Sun et al. used remote sensing images to study the mitigation effect of Beijing water body on urban heat island. The study found that the relationship between the location of water body and the surrounding development land played an important role in the urban coolingisland effect. With the increase of water area, the intensity of cooling island increased, but the efficiency of cooling island decreased significantly.59 % of the water cooling island range was within 100 m, the average intensity of cooling island was 0.54°C·hm-2, and the average efficiency of cooling island was 1.76 °C·(100m)-1·hm-2, and the efficiency of cooling island in small water bodies varied greatly, indicating that the efficiency of cooling island in water bodies had area threshold and other control factors[9]. Adams also found that the 35 m wide river can reduce the temperature around it by 1 ~ 1.5 °C, the effect is stronger when there is green space[10]. Cao et al. studied the intensity of mitigating heat island effect of green space in Nagoya, Japan by remote sensing images. The results showed that the larger the green space area, the stronger the ability of cooling island effect of green space[11].

However, there are few studies on how the dynamic process of urbanization and urban agglomeration affects regional blue-green spatial change, especially

116 the corresponding LST model, especially in large spatial scale[12]. The
117 theoretical challenge behind this topic is how (landscape) processes affect
118 regional thermal environments (RTE), which has so far been fully elucidated.
119 Specifically, many studies have shown the impact of different land cover/use
120 patterns on urban coolingisland effect (UCI), but few studies have quantified
121 their impact on regional cooling island effect (RCI) in the dynamic process of
122 blue-green space. In particular, some previous studies have investigated the
123 relationship between land use / land cover change and land surface temperature
124 in the process of urbanization, but rarely quantified the temperature difference
125 in different land cover conversion processes in a specific period, which limits
126 people's understanding of the impact of different land cover conversion
127 processes on regional blue-green spatial pattern and how this process affects this
128 understanding[13,14]. Furthermore, with the rapid expansion of cities, many
129 neighboring cities are socially and economically connected, and infrastructure
130 networks are interconnected, thus forming a huge urban agglomeration [15,16].
131 Therefore, this new form of urbanization needs to quantify the impact of rapid
132 urbanization on regional blue-green space at a larger (regional) scale in detail, so
133 as to alleviate and solve the problems related to the occurrence and diffusion of
134 urban agglomeration heat island effect.

135 Therefore, in view of the shortcomings of previous studies, this study
136 selects the eastern HaiJiang River-Lake Linkage Zone (EJRLLZ) in Huaihe
137 Ecological Economic Belt, the regional city with the most urbanization potential
138 in China (Fig.1). Using Google Earth Engine cloud platform, land use transfer
139 matrix (Markov model) and corresponding spatial analysis methods to answer
140 the following questions: (1) How fast does urbanization and urban
141 agglomeration affect the pattern and evolution of blue-green space and regional
142 thermal environment ? (2) The contribution of land cover dynamics (land cover
143 transfer of different land cover types in a specific period) to regional blue-green
144 spatial change was quantified. (3) It provides scientific basis for the adaptation

of regional land cover change and mitigation of urban agglomeration heat island effect diffusion.

2. Material and methods

2.1 Study area

The EJRLLZ is a transitional climate from temperate to subtropical, with mild climate, moderate rainfall and clear four seasons, which area is about 55900 km2, including four cities (Huaian, Yancheng, Yangzhou, Taizhou) of Jiangsu province and Chuzhou city of Anhui province. Giving full play to the leading role of Huai'an and Yancheng regional central cities, relying on important lake water bodies such as Hongze Lake, Gaoyou Lake and Nansi Lake, coordinating the ecological civilization construction of Haihe River and Lake, and strengthening the docking and interaction with the surrounding areas such as the Yangtze River Delta and the Wanjiang City Belt.

The Huaihe River Ecological Economic Belt is a national strategy. With the rapid development of economy, EJRLLZ has experienced rapid urbanization, corresponding urban population growth and land cover/land use change. More specifically, Huai'an City and Yancheng City, as the core cities of the EJRLLZ, the urbanization rate is increasing. In the process of urbanization, the natural landscape of the cities in the EJRLLZ has a change trend, which also leads to the increasingly serious eastward trend of RTE. At the same time, in this process, isolated and powerful UCIs (cooling island region) gradually fragmented, and regional heat island and RTE problems also appeared (Fig.4-11).

In general, due to Yancheng, Yangzhou and Taizhou in the EJRLLZ belong to the scope of the world-class urban agglomeration (Yangtze River Delta urban agglomeration), the EJRLLZ is bound to be affected by the expansion of the urban agglomeration heat island effect driven by the development of the world-class urban agglomeration, so it is one of the typical areas affected by the rapid urbanization process in China. Understanding the impact of rapid urbanization on the dynamics and evolution of regional blue-green space can not

only provide policy guidance for the Huaihe River Ecological Economic Belt, but also provide a theoretical basis for the planning of China and other metropolitan areas in the world.

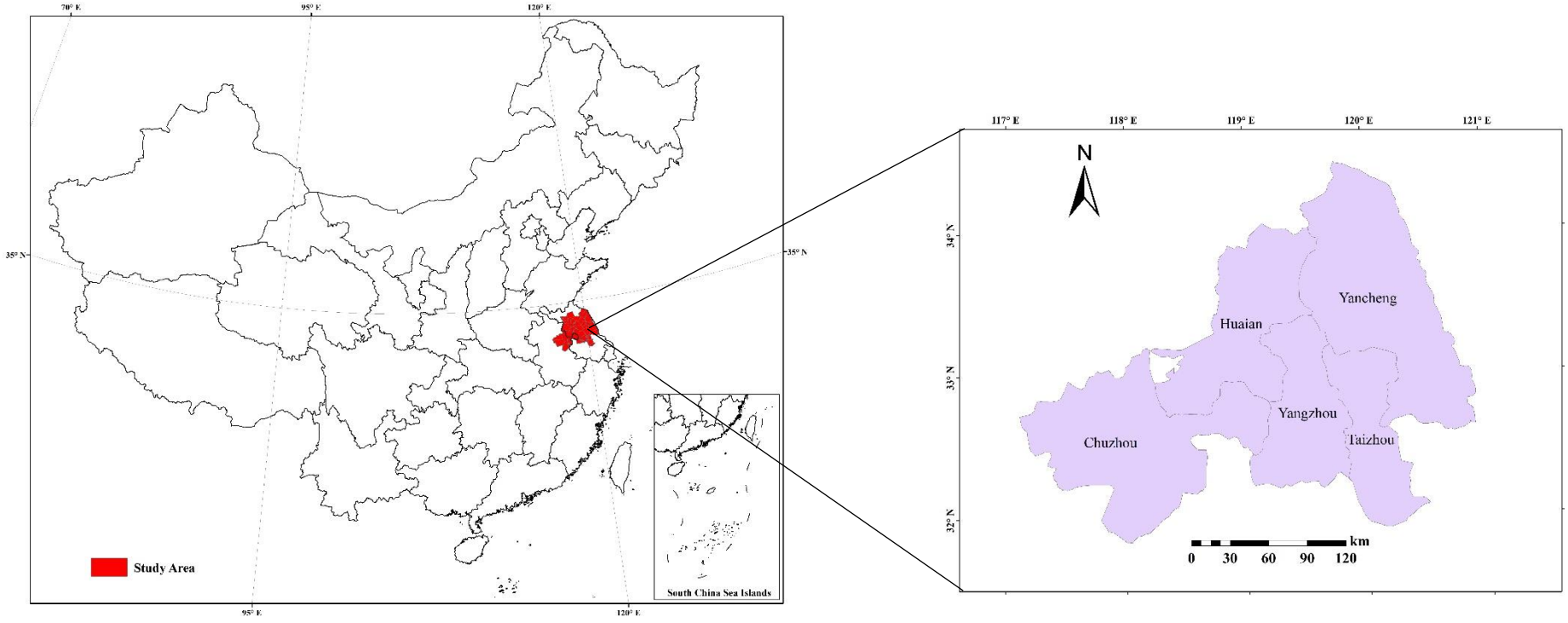

1 Fig.1 Study area

2.2 Data collection and processing

2.2.1 MODIS land surface temperature and Globe land cover data

MODIS Terra/Aqua Global Monthly Mean Land Surface Temperature Products (MOD11A1/MYD11A1 V6) with Spatial Resolution of 1km from 2000 to 2020, which provides daily land surface temperature (LST) and emissivity values in a 1200×1200 kilometer grid. The temperature value is derived from the MOD11_L2 swath product. Above 30 degrees latitude, some pixels may have multiple observations where the criteria for clear-sky are met. When this occurs, the pixel value is the average of all qualifying observations. Provided along with both the day-time and night-time surface temperature bands and their quality indicator layers are MODIS bands 31 and 32 and six observation layers.

The map, known as GlobeLand30 (www.globallandcover.com), comprises data sets collected at 30-metre resolution — more than ten times that of previous data sets. These data sets will be valuable for monitoring environmental changes and for resource management at global, regional and local scales. The GlobeLand30 data sets are freely available and comprise ten types of land cover, including forests, artificial surfaces and wetlands, for the years 2000 and 2010. They were extracted from more than 20,000 Landsat and Chinese HJ-1 satellite images[17]. In this paper, the standard deviation classification method [18] is used to classify the land surface temperature. According to the formula (1), the land surface temperature is divided into seven categories, and the threshold value of the 7-level surface temperature is obtained (see table 1).

$$Q = T \pm x \times s \qquad (1)$$

where Q is different levels of land temperature threshold, T represents average land surface temperature, s means variance of land surface temperature, x denotes the multiple of variance.

Table 1 Classification of land surface temperature

Rank	Temperature threshold
Extremely low temperature zone	Q≤T-2.5s
Low-temperature zone	T-2.5s<Q≤T-1.5s
Sub-low temperature zone	T-1.5s<Q≤T-0.5s
Medium temperature zone	T-0.5s<Q≤T+0.5s
Sub-high temperature zone	T+0.5s<Q≤T+1.5s
High-temperature zone	T+1.5s<Q≤T+2.5s
Extremely high temperature zone	T+2.5s<Q

2.2.2 Calculation of relative land surface temperature from 2000 to 2020

The relative land surface temperature (RLST) can be used to determine the contribution of different regions to the thermal environment, so as to compare the surface temperature differences between different years[19]. RLST equation is:

$$RLST_j^i = LST_j^i - \bar{LST}_j \quad (2)$$

where i represents every year of ten years, LST_j^i represents the pixel remote sensing LST in the j year, $\bar{LST}_j$ denotes the average LST of the whole region. In this study, according to a previous study[20],the region with RLST below 0 °C is defined as a low temperature zone, or we call it a regional cooling island (RCI), the region with RLST above 2 °C is defined as a high temperature zone, or we call it a regional heat island (RHI).

2.3 Dynamic detection of land cover

In this study, land use transfer matrix (LUTM) method (Markov model) was used to detect the dynamic and evolution of land cover from 2000 to 2020. LUTM method originates from the quantitative description of system state and state transition in system analysis. In general, as shown in table 2, T_k represents land cover changes for each period, and X_1 and X_2 are the beginning and end stages of the period, respectively. Qnn represents the area of surface cover S_n in X_1, and

converted to land cover S_n in X_2. Then Q_{n+} and Q_{+n} represent the total area of land cover S_n in X_1 and X_2, respectively[21]. In addition, a difference value will be calculated to determine the general change of indicators during this period.

Table 2 Matrix Formula of Land Use Transfer

T_k		X_1					
		S_1	S_2	S_3	…	S_m	Total
X_2	S_1	Q_{11}	Q_{21}	Q_{31}	⋯	Q_{n1}	Q_{+1}
	S_2	Q_{12}	Q_{22}	Q_{32}	⋯	Q_{n2}	Q_{+2}
	S_3	Q_{13}	Q_{23}	Q_{33}	⋯	Q_{n3}	Q_{+3}
	…	…	…	…	…	…	…
	S_n	Q_{1n}	Q_{2n}	Q_{3n}	⋯	Q_{nn}	Q_{+n}
	Total	Q_{1+}	Q_{2+}	Q_{3+}	⋯	Q_{n+}	
	Total Changes	Q_{1+}-Q_{11}	Q_{2+}-Q_{22}	Q_{3+}-Q_{33}	⋯	Q_{n+}-Q_{nn}	
	Difference	Q_{+1}-Q_{1+}	Q_{+2}-Q_{2+}	Q_{+3}-Q_{3+}	⋯	Q_{+n}-Q_{n+}	

2.4 Evaluation of the impact of land cover dynamics on LST

By calculating the RLST changes of each land cover conversion in different periods, the influence of land cover dynamics on RTE mode and evolution is evaluated[22]. The equation is as follows:

$$T\_DIFF = R\bar{L}ST_s^{x2} - R\bar{L}ST_s^{x1} \quad (3)$$

where T_DIFF represents the RLST difference of each land cover conversion in each period, s is land cover transition type, $x1$ represents the beginning stage of the cycle, $x2$ represents the end stage. Therefore, the positive value of T_DIFF means that the RLST of land cover conversion type increases during this period, and the negative value of T_DIFF means that the RLST decreases.

3. Results

3.1 Dynamics of land cover from 2000 to 2020

The classification results of land cover from 2000 to 2020 are shown in Fig.2, and the ratio and change of land cover types in different regions are shown in Fig.3. The results show that the development land expanded rapidly from 2000 (7.18%) to 2020 (13.55%), mainly concentrated in the urban centers of the EJRLLZ.

Fig.2 also shows that the development land of each city in 2000 was isolated, and the expansion of development land from 2000 to 2020 mainly occurred in the urban centers and suburbs within the administrative boundaries of each city. Subsequently, the isolated heat 'islands' were gradually connected to form a regional heat island, with regional cities expanding from 2010 to 2020, especially Yangzhou and Taizhou, which belong to the Yangtze River Delta urban agglomeration. The water body and arable land patches around the EJRLLZ are obviously distributed. There are many small patches of water in the northeast of Gaoyou Lake in the whole region, which gradually fragmented during 2000-2020. The fragmentation in 2020 is the most serious, which is obviously caused by the rapid development of urbanization between cities and the expansion of urban agglomeration heat island effect. In addition, it is obvious that human activities are mainly affected by river and terrain distribution.

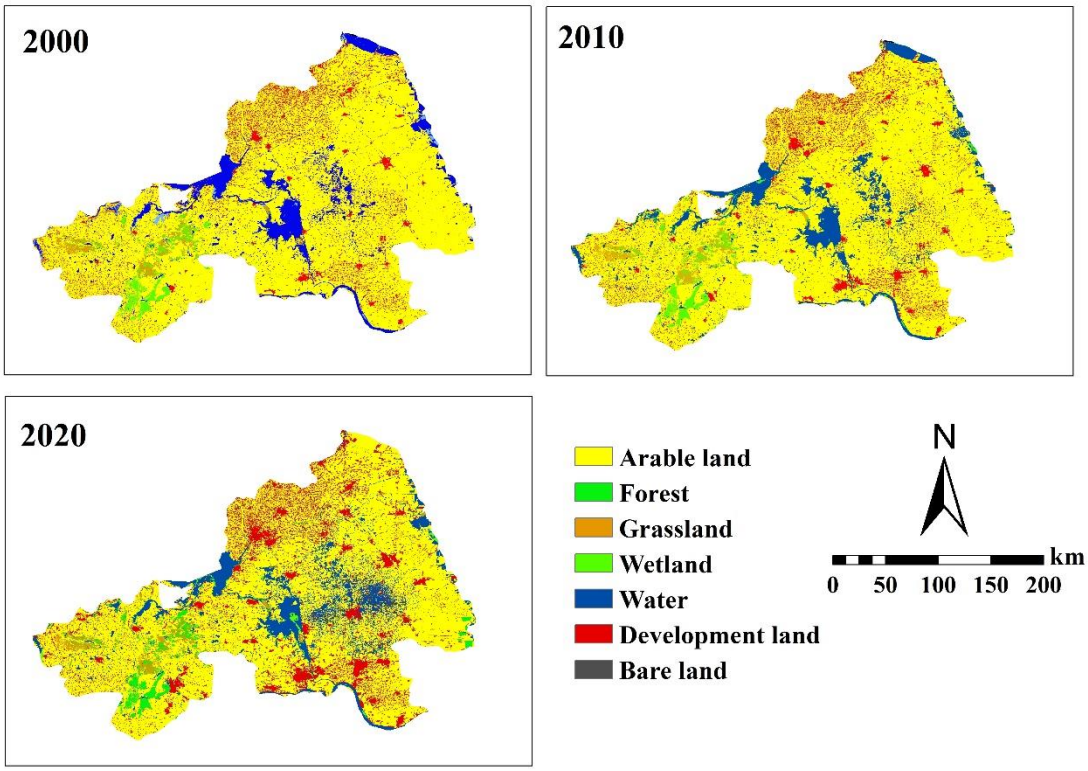

Fig.2 Distribution of land cover types in different years

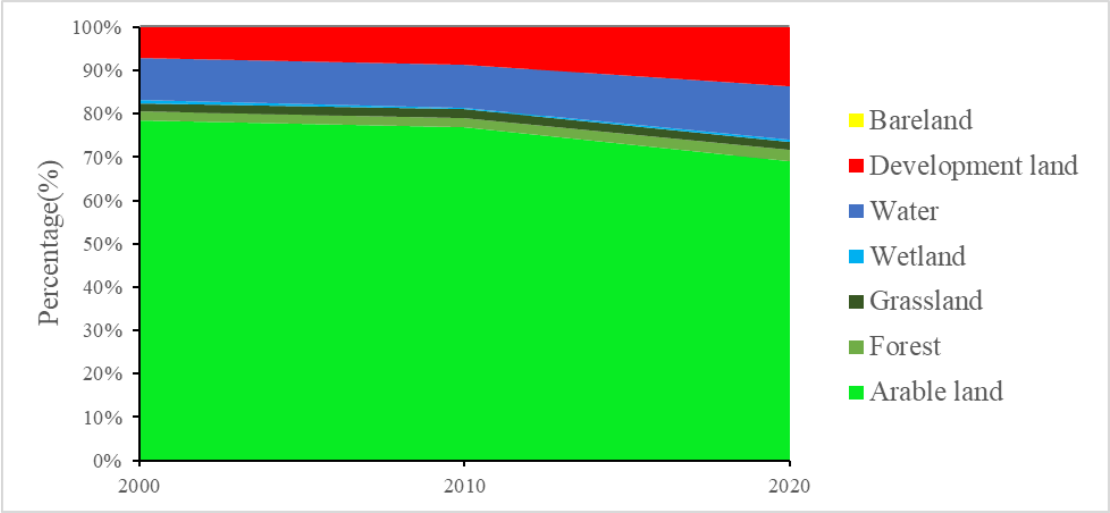

Fig.3 Changes in land coverage rate from 2000 to 2020

Specifically (Tables 3-4), the dynamic trends of land cover changes in T1 (2000-2010) and T2 (2010-2020) are similar, which is also the period of rapid urbanization and the formation of urban agglomerations and the high proportion of blue-green space in the region to maintain a high coolingisland effect. During these 20 years, the change of development land was the largest, and T1 and T2 increased by 687.99 km2 and 2429.64 km2, respectively, mainly from arable land. In addition, development land accounted for the largest proportion (3.26 % and 7.46%, respectively) of the conversions caused by arable land. At the same time, grasslands have also suffered losses, particularly during the T2 period, which may be partially affected by the conversion project since 2002. There was an obvious dynamic relationship between grassland and forest land. From 2000 to 2010, 51.67 km2 grassland became forest land, and from 2010 to 2020, 112.27 km2 grassland became forest land. From 2010 to 2020, development land and water increased rapidly, mostly from arable land. However, the EJRLLZ has experienced another wave of urban expansion and agglomeration in T2, mainly contributed by arable land (7.46%), which means that the region faces rapid urban expansion and agglomeration from 2010 to 2020. In general, development land and water increased rapidly from 2000 to 2020, and the overlong arable land decreased (Table 5). During this period, arable land contributed most to urban expansion (56.92%), followed by water (1.92%) and grassland (0.44%). Over the years, arable land suffered a huge recession, most of which became grassland (9.83%), followed by water (6.07%). At the same time, 121.96km2 (41.24%) of wetland and 55.12km2 (5.97%) of grassland have become water. The land cover transfer matrix from 2000 to 2020 shows that the land use dynamics among arable land, water and development land in the past 20 years are the most significant dynamic process in EJRLLZ. Therefore, these landscape dynamic processes are very important for RTE model and evolution.

113 Table 3 Results of land cover transfer matrix (2000-2010)

T1		2000														
		Arable land		Forest		Grassland		Wetland		Water		Development land		Bare land		Total
		km²	%	km²	%	km²	%	km²	%	km²	%	km²	%	km²	%	km²
2010	Arable land	36069.39	93.92	166.64	15.78	36.87	4.08	85.45	28.69	693.44	14.56	590.56	16.79	0.1	3.07	**37642.45**
	Forest	182.95	0.48	807.1	76.37	51.67	5.57	2.89	0.97	13.52	0.28	3.15	0.09	0.07	2.17	**1061.35**
	Grassland	191.79	0.5	48.59	4.61	692.4	75.01	7.13	2.39	28.01	0.59	5.82	0.17	0.92	26.99	**974.66**
	Wetland	13.98	0.04	8.15	0.77	41.75	4.51	75.72	25.43	48.7	1.03	2.01	0.06	0	0	**190.31**
	Water	686.57	1.79	11.1	1.78	77.84	8.42	124.93	42.15	3937.34	82.75	29.48	0.84	0.01	0.08	**4867.27**
	Development land	1251.59	3.26	7.22	0.68	21.32	2.31	1.06	0.36	37.8	0.79	2885.58	82.05	0.04	1.11	**4204.61**
	Bare land	1.77	0.01	0.05	0.01	0.87	0.1	0.03	0.01	0	0	0.02	0	2.26	66.58	**5**
	Total	**38398.04**	100	**1048.85**	100	**922.72**	100	**297.21**	100	**4758.81**	100	**3516.62**	100	**3.4**	100	
	Total Changes	2328.65	6.08	241.75	23.63	230.32	24.99	221.49	74.57	821.47	17.25	631.04	17.95	1.14	33.42	
	Difference	-755.59		12.5		51.94		-106.9		108.46		687.99		1.6		

114

115

116

117

Table 4 Results of land cover transfer matrix (2010-2020)

T2		2010														
		Arable land		Forest		Grassland		Wetland		Water		Development land		Bare land		Total
		km²	%	km²	%	km²	%	km²	%	km²	%	km²	%	km²	%	km²
2020	Arable land	32310.81	85.85	68.21	6.43	69.35	7.12	34.04	17.97	852.6	17.49	455.86	10.85	0.91	17.62	**33791.78**
	Forest	266.02	0.71	845.55	79.68	112.27	11.52	0.13	0.09	17.17	0.35	4.15	0.1	0.21	4.04	**1245.5**
	Grassland	123.89	0.33	99.61	9.39	706.27	72.46	0.27	0.14	15.03	0.31	5.74	0.14	1.67	32.42	**952.48**
	Wetland	24.25	0.06	1.64	0.16	1.89	0.19	92.1	48.18	160.43	3.29	0.47	0.01	0	0	**280.78**
	Water	2099.69	5.58	37.88	3.57	61.5	6.31	59.82	31.73	3735.61	76.72	29.65	0.71	0.36	6.89	**6024.51**
	Development land	2806.4403	7.46	7.08	0.67	18.3	1.89	3.62	1.89	89.73	1.84	3707.72	88.19	0.35	6.85	**6633.2403**
	Bare land	1.53	0.01	1.05	0.1	4.95	0.51	0	0	0.05	0	0.01	0	1.67	32.18	**9.26**
	Total	**37632.6303**	**100**	**1061.02**	**100**	**974.53**	**100**	**189.98**	**100**	**4870.62**	**100**	**4203.6**	**100**	**5.17**	**100**	
	Total Changes	5321.8203	14.15	215.47	20.32	268.26	27.54	97.88	51.82	1135.01	24.28	495.88	11.91	3.5	67.82	
	Difference	-3840.8503		184.48		-22.05		90.8		1153.89		2429.6403		4.09		

123 Table 5 Results of land cover transfer matrix (2000-2020)

T3		2000														
		Arable land		Forest		Grassland		Wetland		Water		Development land		Bare land		Total
		km²	%	km²	%	km²	%	km²	%	km²	%	km²	%	km²	%	km²
2020	Arable land	31678.01	82.5	163.14	15.44	105.89	11.48	79.52	26.73	1000.62	21.02	764.24	21.73	0.32	9.39	**33791.74**
	Forest	358.25	0.94	747.81	70.76	118.72	12.87	1.3	0.64	13.33	0.27	5.86	0.17	0.23	6.84	**1245.5**
	Grassland	217.35	0.57	105.4	9.98	585.07	63.41	14.09	4.93	23.88	0.39	5.11	0.15	1.59	46.65	**952.49**
	Wetland	28.01	0.08	6.73	0.64	23.94	2.61	73.43	24.74	147.37	3.48	1.31	0.06	0	0	**280.79**
	Water	2330.6	6.07	18.64	1.77	55.12	5.97	121.96	41.24	3440.61	72.16	57.43	1.63	0.16	4.66	**6024.52**
	Development land	3775.95	9.83	13.68	1.3	28.88	3.14	5.03	1.71	127.8	2.68	2681.97	76.26	0.17	4.95	**6633.48**
	Bare land	2.15	0.01	1.12	0.11	4.83	0.52	0.03	0.01	0.17	0	0	0	0.93	27.51	**9.23**
	Total	**38390.32**	100	**1056.53**	100	**922.45**	100	**295.36**	100	**4753.78**	100	**3515.92**	100	**3.4**	100	
	Total Changes	6712.31	17.5	308.72	29.24	337.38	36.59	221.93	75.26	1313.17	27.84	833.95	23.74	2.47	72.49	
	Difference	-4598.58		188.97		30.04		-14.57		1270.74		3117.56		5.83		

124

3.2 Land surface temperature trends from 2000 to 2020

Overall, the LST pattern and evolution from 2000 to 2020 have a similar trend with land cover dynamics. Fig.4-11 and table 6 show the average land surface temperature (LST) and relative land surface temperature (RLST) of MODIS in four seasons. The average, maximum and minimum values of summer land surface temperature in 2020 are the highest, which are 31.81 °C, 39.94 °C and 25.09 °C, respectively, and are gradually increasing from 2000 to 2020. The average, maximum and minimum values of spring surface temperature in 2010 were the lowest, which were 19.61 °C, 27.07 °C and 11.77 °C, respectively. The lowest value of autumn average was 21.05 °C in 2000, and the lowest value of autumn maximum and minimum was still 27.91 °C and 12.61 °C in 2010. The lowest values of winter average and maximum were 10.22 °C and 13.36 °C in 2000, while the lowest value of winter minimum was 2.43 °C in 2010. Urban cooling island effect is the strongest in winter, followed by autumn, summer heat island effect is the strongest.

The results of Fig.4-11 show that the regional coolingisland effect (RCI) is gradually isolated and RHI is significantly enhanced except Hongze Lake and Gaoyou Lake, especially in the urban and urban districts of the EJRLLZ. Since 2000, several isolated urban heat islands have gradually merged, which may be due to the integration of Chuzhou, Yangzhou, Taizhou and Nanjing metropolitan area, resulting in the increasing land coverage of development land. From 2000 to 2020, the RHI around the Yangtze River estuary continued to expand, but some RHI in the north of the EJRLLZ decreased, especially in the low RLST area. These mitigation trends in recent years may be caused by the so-called ecological red line project and greenway network construction implemented by local governments in the EJRLLZ.

Spring (March-May): Seasonal variation of urban land surface temperature spatial pattern in the EJRLLZ in spring is shown in Fig.4-5. Three years (2000, 2010, 2020) cooling island intensity in the spatial variation range is roughly the same, are concentrated in Hongze Lake, Gaoyou Lake. In terms of the overall and local spatial pattern changes, the urban area as a whole shows the heat island effect, which is not very obvious in the region, and the cooling island effect is the main advantage. The spatial pattern of heat island in different years is quite different in different seasons. The cooling island effect in Yangzhou and Taizhou in 2000 is significantly higher than that in 2010 and 2020. The heat island effect and the range of heat island in Chuzhou gradually increased from 2000 to 2020. It is worth noting that the heat island effect of Chuzhou in spring is stronger than other cities in the whole four seasons. The heat island effect of Huai'an, Taizhou and Yangzhou is more and more concentrated in the urban area.

Summer (June-August): The main reason for the highest temperature season in a year is the maximum solar radiation absorbed by the surface and sunshine hours provide good conditions for the increase of LST. Seasonal variation of urban land surface temperature spatial pattern in EJRLLZ in summer is shown in Fig.6-7. In terms of the spatial variation range of cooling island intensity (the maximum and minimum values of cooling island intensity), the spatial variation range of cooling island intensity in the three years (2000, 2010, 2020) is roughly the same, which is concentrated in Hongze Lake and Gaoyou Lake. In terms of the change of the overall and local spatial pattern of the cooling island, the city as a whole presents the heat island effect. The spatial pattern of the heat island in different years is quite different in urban areas in different seasons. The cooling island effect in Yangzhou and Taizhou in 2000 is significantly higher than that in 2010 and 2020. The intensity and scope of Yancheng heat island in 2010 were significantly higher than in 2000 and 2020. The urban heat island effect of Yancheng, Huai'an, Yangzhou and Taizhou in 2010 was more concentrated in urban areas than in 2000 and 2020, and the spatial pattern of urban heat island was very different in the three years (The urban heat island effect of Chuzhou in 2000 was significantly higher than that in 2010 and 2020. The cooling island effect of Chuzhou in 2020 was significantly higher than that in 2010 and 2000).

Autumn (September-November): LST began to decrease, which was mainly affected by the reduction of solar radiation, the shortening of sunshine time, and the reduction of vegetation coverage. Therefore, LST began to decrease again. Seasonal variation of urban land surface temperature spatial pattern in EJRLLZ in autumn is shown in Fig.8-9. The spatial variation range of cooling island intensity in three winter years (2000, 2010, 2020) accounted for a large area in the region. The regional cooling island effect in 2000~2020 tends to be the area of five city boundaries year by year, mainly distributed in the lakes with large cooling island effect in the region: Hongze Lake and Gaoyou Lake.

Winter (December-February): As the temperature drops further, it is winter wheat overwintering period, crop growth is slow, so the land cover type presents contiguous low value area. The interannual variation of the spatial pattern of land surface temperature in the EJRLLZ of winter is shown in Fig.10-11. The spatial variation range of cooling island intensity (the maximum and minimum of cooling island intensity) in the three winter years (2000, 2010, 2020) is very similar, which is larger than that in autumn. In terms of the seasonal changes of the overall and local spatial patterns, in general, the winter region from 2000 to 2020 showed the cooling island effect as a whole, but compared with autumn, the cooling island phenomenon was more common. The spatial pattern of cooling island in different years is quite different in the region (the intensity of cooling island in Yancheng in 2010 is significantly greater than that in 2000 and 2020. In 2000, the intensity of heat island in Chuzhou City was significantly lower than that in 2010 and 2020). In addition, the range of regional cooling islands in the

three years was relatively concentrated in 2000 and 2010, and gradually dispersed into fragmentation distribution in 2020.

It can be seen that the LST distribution in different months is closely related to the seasonal changes of solar radiation, sunshine time, LUCC type and vegetation coverage in this period. Therefore, the LST value and RLST value in the study area are in the order of summer > autumn > spring > winter, except that Chuzhou has the strongest heat island effect in spring. In general, the average LST in EJRLLZ has a strong spatial variability, and the seasonal variation of land surface temperature is mainly determined by climate factors, LUCC coverage and spatial pattern changes. Overall, the spatial pattern of heat island in different seasons is quite different among different cities in regional cities. Because there are a large number of water bodies (lakes and rivers) and green space (arable land) in the region, there are relatively fixed cooling island areas in any season in the region, and these cooling island areas are directly corresponding to the area where the water body is located, mainly the land surface temperature of the water body is far lower than the land surface temperature of the surrounding impervious layer.

225 Table 6 The lowest, highest and average land surface temperatures of four seasons in different years

Year	MODIS Land Surface Temperature(℃)															
	Spring				Summer				Autumn				Winter			
	T_{mean}	T_{max}	T_{min}	StdDev	T_{mean}	T_{max}	T_{min}	StdDev	T_{mean}	T_{max}	T_{min}	StdDev	T_{mean}	T_{max}	T_{min}	StdDev
2000	22.54	28.76	13.64	2.14	29.68	37.38	24.49	1.38	21.05	29.01	21.05	1.1	10.22	13.36	5.29	1.09
2010	19.61	27.07	11.77	1.74	30.51	38.38	24.61	1.49	22.24	27.91	12.61	1.49	10.25	14.11	2.43	1.65
2020	23.51	32.28	14.92	2.51	31.81	39.94	25.09	2.0	24.17	30.55	18.46	1.34	11.21	14.99	4.7	1.31

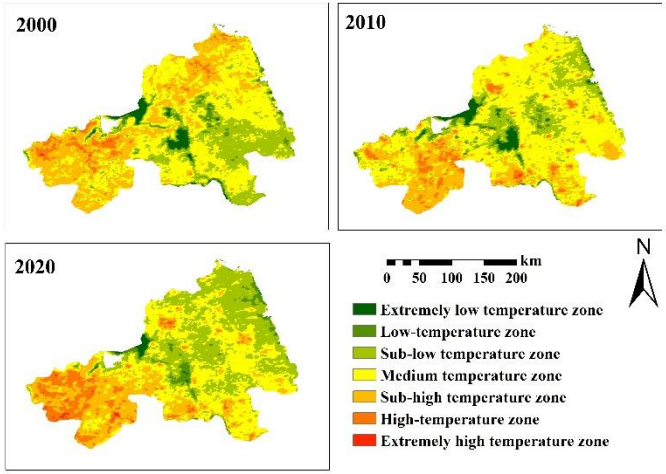

Fig.4 Classification of land surface temperature in spring in different years

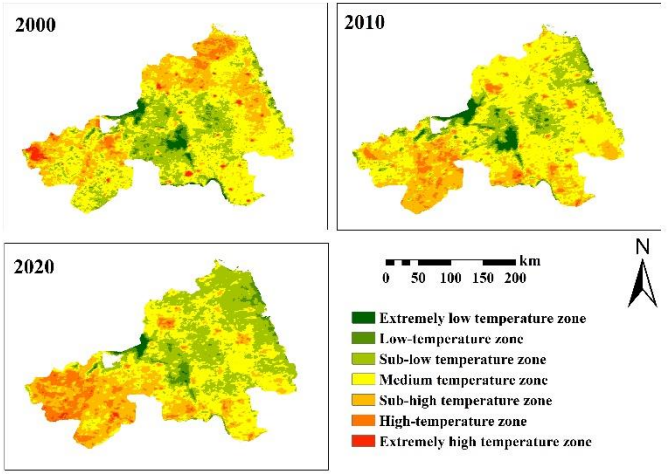

Fig.6 Classification of land surface temperature in summer in different years

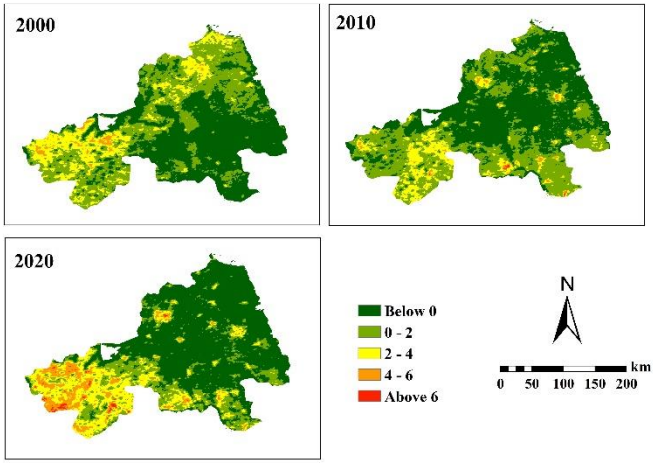

Fig.5 Classification of relative land surface temperature in spring in different years

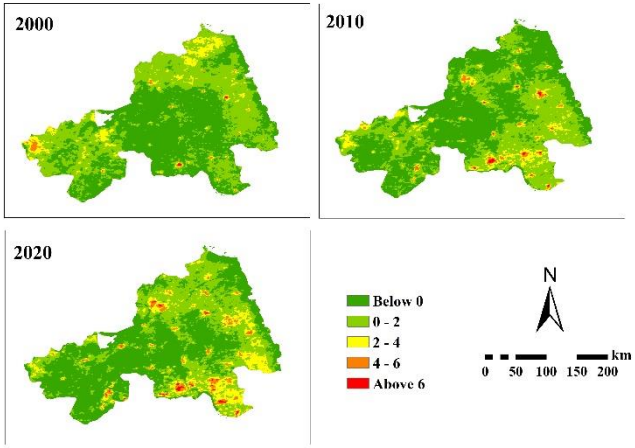

Fig.7 Classification of relative land surface temperature in summer in different years

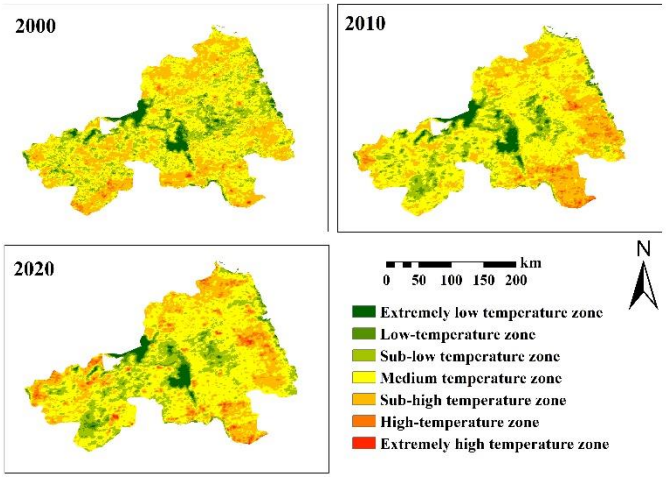

Fig.8 Classification of land surface temperature in autumn in different years

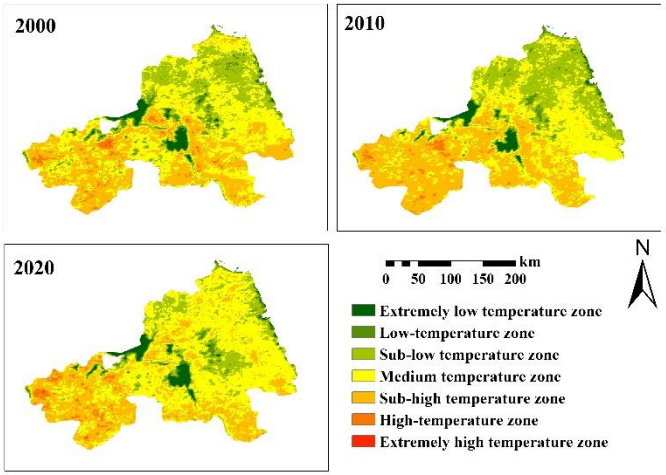

Fig.10 Classification of land surface temperature in winter in different years

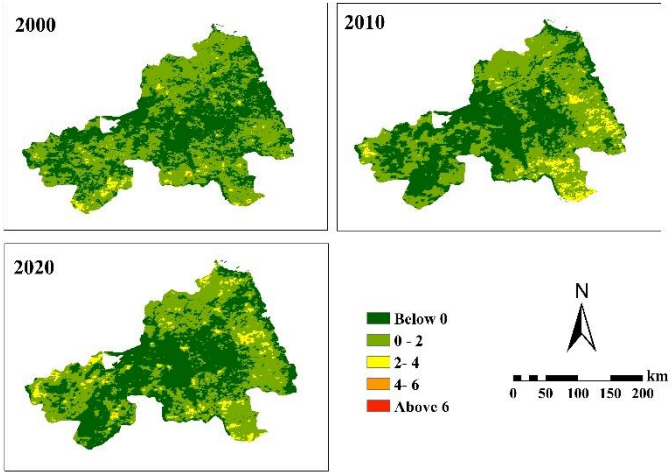

Fig.9 Classification of relative land surface temperature in autumn in different years

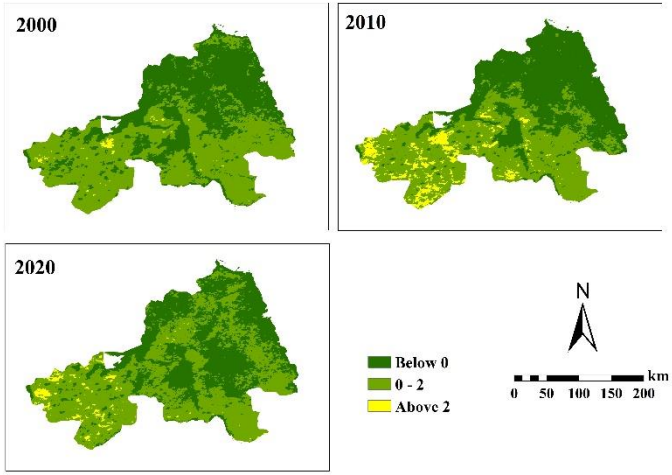

Fig.11 Classification of relative land surface temperature in winter in different years

3.3 Changes and Trends of RLST from 2000 to 2020

Table 7 shows that the average RLST of water and wetland in four seasons is between -4 °C and -1 °C, the average RLST of arable land in four seasons is between 0 °C and 1 °C, the average RLST of woodland in four seasons is between -1.5 °C and 1.58 °C, the average RLST of grassland in four seasons is between -0.96 °C and 2 °C, and the average RLST of bare land in four seasons is between -1 °C and 2 °C. The average RLST of development land is between -0.08 °C in winter of 2010, and the average RLST of spring, summer and autumn is mainly between 0 °C and 2 °C. These results show that urbanized land usually produces heat island effect, while green space and water may produce cooling island effect in different seasons. However, the average RLST in grasslands was -0.96 °C in summer of 2020 and -0.96 °C in autumn of 2010 and 2020, which was different from previous studies[23,24].

According to these results and Peng's definition [25] , forest land, grassland, water and wetland cover types are considered to be ecological land (WA: Water; WE: Wetland; AR: Arable land; FO: Forest; GR: Grassland). Because compared with the DE (Development land) and BA (Bare land), they have the cooling effect. The increase in forest land, grassland, water and wetlands is then referred to as ecological land benefits, including DE-GR、BA-GR、DE-WA、BA-WA、DE-FO and BA-FO(Fig.12). It can be seen that in the process of urbanization and urban agglomeration, the loss of ecological land generally contributes to the increase of temperature, while the increase of ecological land usually reduces the temperature. In addition, the transition from bare land to ecological land significantly reduced RLST. For the conversion between woodland, grassland, water and wetland, the general model is that the land coverage transferred to woodland, water and wetland reduces RLST, while the land coverage transferred to grassland usually increases RLST.

The results in Tables 8-10 show that the RLST values of all land cover types transferred to wetlands in summer in T1 and T2 are negative. The RLST values of all land cover types transferred to water and grassland in T2 summer were negative. Except that the WA-AR value of T1 land coverage type is positive (0.08 °C) and the DE-AR value of T2 land coverage type is positive (0.38 °C), the rest are all negative in summer. T1 transferred to arable land in autumn was negative except the DE-AR value of land cover type was positive (0.15 °C).

Combined with the results of Fig.12 and Table 8-10, it can be clearly seen that in general, especially in summer, the land cover type transferred to the blue system (water and wetland) can reduce the temperature more than the green system (arable land, forest land and grassland). The RLST values of land cover types transferred to grassland in T1 autumn and T2 summer were negative, and the RLST values of conversion from cropland and woodland to grassland were

mostly negative. This means that although conversion from DE and BA to grassland can reduce temperature, grassland has a lower cooling effect than water and wetlands. In addition, in T1 and T2, the RLST variation of BA and DE's eco-land income is generally less than that of BA and DE's loss. These results show that compared with the cooling effect brought by ecological land, the loss of ecological land, especially the type of forest land coverage, will significantly increase the regional temperature. The difference of RLST between ecological land loss and ecological land income is of great significance for ecological land protection.

The results in Tables 8-10 show that the RLST values of all land cover types transferred to wetlands in summer T3 are negative except that the FO-WE value of land cover types is positive (0.06 °C). The RLST values of all land cover types transferred to farmland and woodland in summer of T3 were negative. The RLST values of all land cover types transferred to grassland in summer of T3 were negative. Except the FO-WA value of T3 land cover type is positive (0.79 °C), the rest are negative. In general, RLST changes and dynamics in different land cover conversions in T3 (2000-2020) are similar to those in specific periods (T1 and T2). It can be determined that DE and BA are the dominant factors of thermal environment, DE and BA affect the thermal environment effect of land conversion. Development land expansion or urbanization increases regional temperature and leads to RHI. All the land cover types transferred to the blue system will reduce the temperature, among which GR-WE (-139 °C) and BA-WA (-1.4 °C) have larger negative RLST. It can be seen that the transformation to water and wetland usually reduces the temperature, and vice versa, which means that water will be the best choice for the regional climate adaptation. The model of T3 (2000-2020) is similar to T1 and T2 mentioned above. In particular, the RLST results from 2000 to 2020 again show that the RLST changes of ecological land income from BA and DE are generally less than the loss of BA and DE. The results show that the existing ecological land (especially water) is very valuable for climate adaptation, because the ecological land transformed from DE or BA cannot provide such a huge cooling effect as the existing nature.

Table 7 Average relative land surface temperature in four seasons of different land cover types in different years

Land cover	2000				2010				2020			
	Spring	Summer	Autumn	Winter	Spring	Summer	Autumn	Winter	Spring	Summer	Autumn	Winter
Arable land	0.25	0.11	0.15	0.16	0.14	0.1	0.27	0.23	0.08	0.13	0.17	0.63
Forest	1.22	0.25	0.01	0.84	1.58	-0.46	-1.24	1.26	1.25	-1.5	-1.18	0.72
Grassland	1.84	0.95	0.06	0.74	1.61	0.16	-0.53	1.33	1.95	-0.96	-0.52	1.25
Wetland	-1.83	-1.11	-1.52	-1.4	-2.55	-1.57	-2.44	-1.93	-2.57	-2.86	-2.09	-2.48
Water	-3.43	-1.92	-1.6	-1.7	-2.69	-1.73	-2.57	-2.39	-2.17	-2.14	-1.6	-1.76
Development land	0.75	0.96	0.55	0.02	0.95	1.11	0.81	-0.08	1.1	1.77	0.96	0.16
Bare land	0.23	0.23	-0.15	0.28	0.36	-0.03	-0.9	0.52	1.57	-0.68	-0.51	0.31

309

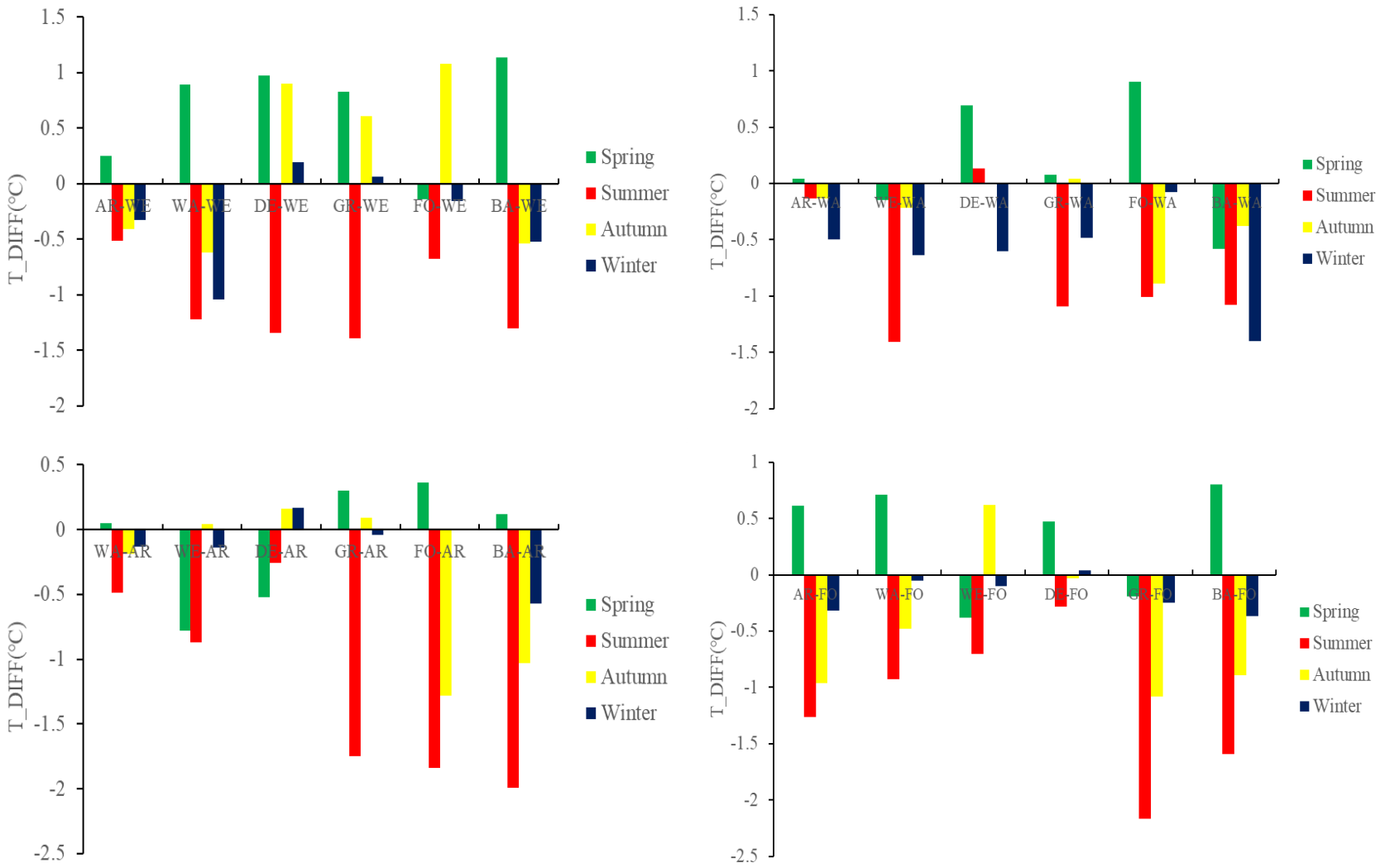
T_DIFF(°C)
1.5
1
0.5
0
-0.5
-1
-1.5
-2
AR-WE
WA-WE
DE-WE
GR-WE
FO-WE
BA-WE
Spring
Summer
Autumn
Winter
AR-WA
WE-WA
DE-WA
GR-WA
FO-WA
BA-WA
WA-AR
WE-AR
DE-AR
GR-AR
FO-AR
BA-AR
AR-FO
WA-FO
WE-FO
DE-FO
GR-FO
BA-FO
-2.5

310

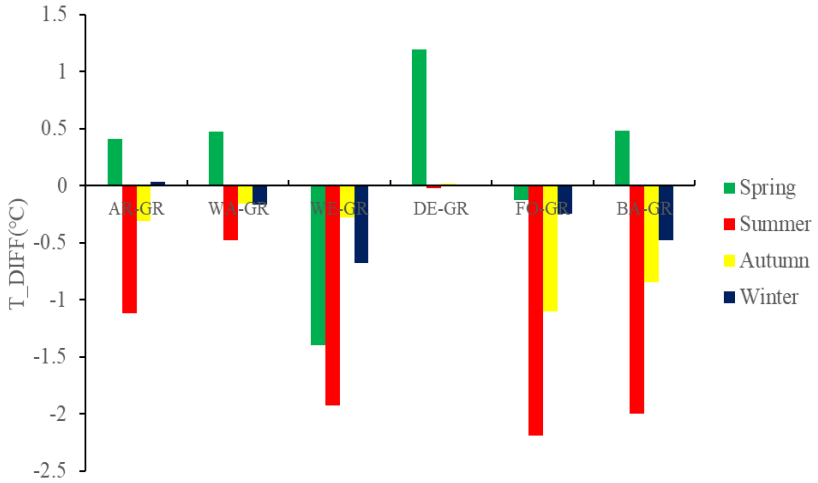

311

312 Fig.12 Relative land surface temperature changes in the transfer of ecological land types

313

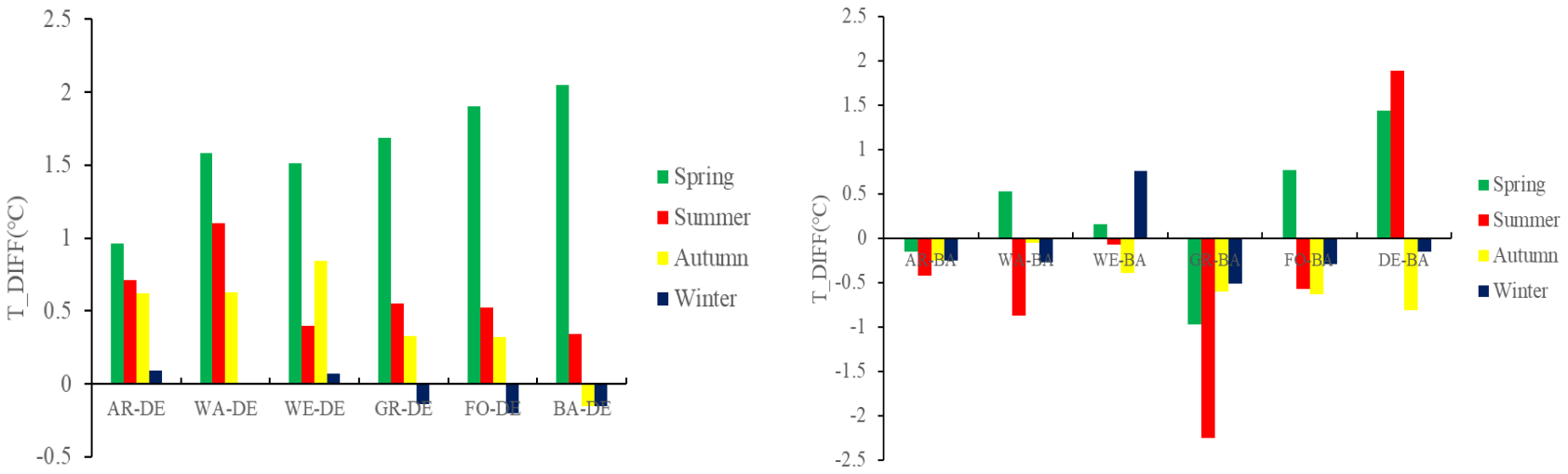

314

315 Fig.13 Relative land surface temperature changes in the transfer of other types

316

317 Table 8 Changes of relative land surface temperature in different land cover types transferred to blue system (T_DIFF)

Land Cover Conversion	T1 (2000-2010)				T2 (2010-2020)				T3 (2000-2020)			
	T_DIFF (℃)				T_DIFF (℃)				T_DIFF (℃)			
	Spring	Summer	Autumn	Winter	Spring	Summer	Autumn	Winter	Spring	Summer	Autumn	Winter
Unchanged WA	0.78	0.11	-1,17	-0.88	0.1	-1.09	0.52	0.13	0.83	1.02	-0.61	-0.72
AR-WA	0.46	0.17	-0.34	-0.21	-0.37	-0.54	-0.03	-0.37	0.04	-0.13	-0.13	-0.5
WE-WA	-0.64	-0.22	-1.06	-0.58	-0.19	-1.42	0.74	0.22	-0.15	-1.41	-0.22	-0.64
DE-WA	1.43	0.95	0.25	-0.16	-0.35	-0.4	-0.06	-0.24	0.69	0.13	0.01	-0.6
GR-WA	-0.74	-0.28	0.11	0.28	-0.17	-0.79	0.32	-0.57	0.08	-1.09	0.04	-0.48
FO-WA	0.26	-0.13	-1.17	0.39	1.2	-0.61	0.27	-0.51	0.9	-1.01	-0.89	-0.08
BA-WA	-0.7	0.17	-0.85	-0.35	-0.27	-1.7	0.47	-0.54	-0.58	-1.08	-0.38	-1.4
Unchanged WE	0.19	-0.23	-0.3	-0.28	-0.01		0.73	-0.11	-0.2	-1.38	0.41	-0.36
AR-WE	-0.3	-0.11	0.23	0.49	-0.12	-0.62	0.31	-0.44	0.25	-0.51	-0.41	-0.33
WA-WE	0.36	-0.19	-1.09	-1.16	0.7	-1.35	0.8	0.12	0.89	-1.22	-0.62	-1.04
DE-WE	-0.39	-0.42	-0.03	0.56	0.67	-0.69	0.53	-0.32	0.97	-1.34	0.9	0.19
GR-WE	-0.51	-0.19	-0.61	-0.34	0.79	-0.8	0.86	-0.22	0.83	-1.39	0.61	0.06
FO-WE	-1.67	0.06	-0.16	0.19	1.7	-0.15	0.78	-0.47	-0.14	-0.68	1.08	-0.16
BA-WE				0	-0.68	-2.78	0.84	0	1.14	-1.3	-0.54	-0.52

318

319

320

321

322

323 Table 9 Changes in relative surface temperature over land cover types transferred to green systems (T_DIFF)

Land Cover Conversion	T1 (2000-2010)				T2 (2010-2020)				T3 (2000-2020)			
	T_DIFF (℃)				T_DIFF (℃)				T_DIFF (℃)			
	Spring	Summer	Autumn	Winter	Spring	Summer	Autumn	Winter	Spring	Summer	Autumn	Winter
Unchanged AR	-0.12	0.01	0.14	0.08	-0.01	0.14	-0.1	0.02	-0.21	0.08	0.04	0.12
WA-AR	0.13	0.08	-0.29	-0.15	-0.03	-0.67	0.45	0.12	0.05	-0.49	-0.19	-0.13
WE-AR	-0.02	-0.43	-0.47	-0.44	1.22	-1.01	0.85	-0.1	-0.78	-0.87	0.04	-0.14
DE-AR	-0.32	-0.2	0.15	-0.0001	0.24	0.38	0.01	0.14	-0.52	-0.26	0.16	0.17
GR-AR	-0.29	-0.74	-0.69	0.32	0.58	-0.87	0.2	-0.37	0.3	-1.75	0.09	-0.04
FO-AR	0.14	-0.74	-1.18	0.57	0.26	-1.01	0.07	-0.47	0.36	-1.84	-1.28	-0.01
BA-AR	0.44	-0.58	-1.03	0.25	-0.53	-0.89	0.5	-0.33	0.12	-1.99	-1.03	-0.57
Unchanged FO	0.54	-0.68	-1.31	0.44	-0.33	-1.23	-0.04	-0.62	0.19	-1.93	-1.39	-0.18
AR-FO	0.34	-0.37	-1.04	0.55	-0.42	-0.69	-0.7	-0.25	0.61	-1.26	-0.96	-0.32
WA-FO	-0.2	-0.04	-0.72	0.35	1.42	-0.67	0.11	-0.36	0.71	-0.93	-0.48	-0.05
WE-FO	-0.18	0.38	-0.7	0.32	0.84	-1.13	1.09	-0.24	-0.38	-0.7	0.62	-0.1
DE-FO	0.62	0.37	-0.91	0.39	0.26	0.39	0.25	0.07	0.47	-0.28	-0.03	0.04
GR-FO	-0.13	-0.92	-1.03	0.47	0.13	-1.24	-0.05	-0.69	-0.19	-2.17	-1.08	-0.25
BA-FO	0.59	-0.44	-1.24	0.15	0.02	-1.12	0.12	-0.69	0.8	-1.59	-0.89	-0.37
Unchanged GR	-0.44	-1.05	-0.85	0.52	0.22	-1.2	-0.04	-0.69	-0.32	-2.31	-0.95	-0.19
AR-GR	-0.25	-0.13	-0.45	0.42	0.47	-0.64	0.15	-0.42	0.41	-1.12	-0.31	0.03
WA-GR	0.41	0.52	-0.6	-0.04	0.53	-0.76	0.26	-0.29	0.47	-0.48	-0.16	-0.17
WE-GR	-0.75	0.47	-0.14	0.62	0.69	-0.63	0.91	-0.17	-1.4	-1.93	-0.28	-0.68
DE-GR	0.67	0.54	-0.2	0.17	0.33	-0.04	0.38	-0.18	1.19	-0.02	0.02	0.002
FO-GR	-0.12	-0.92	-1.03	0.46	0.18	-1.19	-0.05	-0.67	-0.13	-2.19	-1.1	-0.25
BA-GR	0.58	-0.18	-0.79	0.46	0.04		-0.004	-0.9	0.48	-2	-0.85	-0.48

Table 10 Changes of relative land surface temperature in non-blue-green space with different land cover types (T_DIFF)

Land Cover Conversion	T1 (2000-2010)				T2 (2010-2020)				T3 (2000-2020)			
	T_DIFF (℃)				T_DIFF (℃)				T_DIFF (℃)			
	Spring	Summer	Autumn	Winter	Spring	Summer	Autumn	Winter	Spring	Summer	Autumn	Winter
Unchanged DE	0.08	-0.09	0.13	-0.13	-0.18	0.5	0.09	0.2	0.03	0.48	0.24	0.06
AR-DE	0.76	0.78	0.55	-0.14	0.45	1.45	0.29	0.03	0.96	0.71	0.62	0.09
WA-DE	1.51	0.87	0.32	-0.31	0.06	0.15	0.53	0.22	1.58	1.1	0.63	0.01
WE-DE	0.88	0.34	0.05	-0.38	1.34	-0.21	0.79	-0.27	1.51	0.4	0.84	0.07
GR-DE	1.31	1.09	0.32	-0.08	0.7	-0.43	0.31	-0.47	1.69	0.55	0.33	-0.14
FO-DE	1.31	1.11	-0.22	0.32	1.02	-0.22	0.63	-0.43	1.9	0.52	0.32	-0.2
BA-DE	2.26	1.85	-0.49	0.4	0.96	-0.01	0.67	-0.58	2.05	0.34	-0.15	-0.15
Unchanged BA	0.6	-0.11	-0.74	0.35	0.05	-1.58	-0.01	-0.94	1.02	-1.84	-0.74	-0.65
AR-BA	0.02	0.12	-0.38	0.74	0.22	0.08	0.04	-0.99	-0.15	-0.42	-0.25	-0.25
WA-BA	0.51	0.7	-0.34	0.44	0.57	-1.14	0.55	-0.31	0.53	-0.87	-0.05	-0.27
WE-BA	0.82	-0.53	-1.21	0.37				0	0.16	-0.07	-0.39	0.76
GR-BA	0.47	-0.27	-0.86	0.4	0.22	-0.75	-0.1	-0.81	-0.97	-2.25	-0.6	-0.51
FO-BA	0.59	-0.72	-0.99	0.24	-0.07	-1.27	0.56	-0.36	0.77	-0.57	-0.63	-0.29
DE-BA	2.2	1.02	-0.94	0.83	0.03	0.07	0.77	-0.12	1.44	1.89	-0.81	-0.15

4. Discussion

4.1 Influence of Rapid Urbanization on Regional Blue and Green Space

It is widely believed that urbanization (and urban agglomerations) significantly reduces UCI effects and increases RTE [5,12-14,26]. In particular, the impact of the model on the UCI effect, such as the study of Weng[4] and Cao[11], has proposed that LST is related to some dominant land cover and land use types within a certain temperature range. Similarly, this study also found that the LST of water and wetland was significantly higher than that of other land coverage types, and the average RLST was mainly between 3 °C and 8 °C. However, the results of this study show that the blue-green space is not only dominated by WA and WE land cover types (as well as urbanization), but also significantly affected by specific land conversion processes (e.g. AR-WA and DE-WE), as well as the difference in the cooling effect of ecological land losses and benefits (Table 8-10, Fig.12). These findings provide new evidence for explaining the rapid urbanization mechanism of UCI. In addition, cities are generally isolated and constrained by administrative boundaries at the initial stages of urbanization, particularly in the context of China. Regional Cooling Island (RCI) is therefore not isolated. In the process of common development of regional cities (Fig.2), the deterioration of RTE makes these connected RCIs gradually isolated (Fig.6 and 7). In addition, climate change and anthropogenic heat emissions are the mechanisms for RCI fragmentation and weakening.

From the beginning of the 21st century, the government of the EJRLLZ has also implemented projects such as returning farmland to forests, ecological red lines and greenway networks. As shown in Fig.4-11, the RCI intensity in the northern part of the EJRLLZ began to rise slightly (2010-2020).

4.2 Impacts on regional climate adaptation planning

Compared with previous studies focusing on a single city in a single period[15,16,27,28], this study uses the LUTM method to quantify the multi-period changes at the regional scale. The research results reveal the general rule of RLST dynamics and evolution in the process of rapid urbanization, and provide a scientific basis for the adaptation and mitigation of rapid urbanization.

The cooling effect of water and wetland found in this study is also consistent with many previous studies[29-34]. However, the cooling effect of grassland needs further analysis. The results of this study (Table 8-10, Fig.12-13) showed that grassland had no cooling effect similar to that of water and wetland. This result is different from previous research results, the previous results show that grassland also has cooling effect[35-37]. In fact, Yu[22] has proposed that

the cooling effect of grass vegetation is greatly affected by its local background climate, which shows that rainfall, irrigation and wind speed conditions can significantly affect the cooling effect of grass vegetation. Kang[38] also pointed out that the expansion of irrigation agriculture reduced the land surface temperature and moistened the surface air, but promoted the comprehensive measurement of temperature and humidity, thereby enhancing the intensity of heat waves. In addition, some studies have found that grassland vegetation may have a positive impact on the thermal environment, thereby impeding the formation of 'cooling island', mainly due to lack of irrigation and difficulty in maintaining 'green state'. Santamouris[23,24] also concluded that the cooling effect of grassland is still uncertain and needs further investigation. Therefore, we believe that grassland is not a good choice to adapt to and mitigate climate change, whether in EJRLLZ or in other climate zones.

The research results (Tables 8-10) also found that water and wetland usually had better cooling effect than woodland, which provided new evidence for discussing the difference in cooling effect between water and woodland[11,39-41]. We suggest that the land coverage of water body should be given priority to in the agglomeration area of the EJRLLZ to alleviate the RHI effect.

In addition, in general, the pattern-process-scale-effect diagram is the basic principle of landscape ecology. It can also explain the dynamics and evolution of thermal environment. The impact of land landscape pattern on urban cooling island (UCI) effect has attracted much attention[29-34], but there is still a lack of understanding of the quantitative impact of land cover process on RTE effect, especially the land cover change process in a specific period [15,16,27]. For example, Sun and Chen[19] found that, the transformation from impervious land to green land has obvious cooling effect, but the expansion from impervious land to green land will lead to significant changes in the internal thermal effect of green land. Yu et al.[42] found in Fuzhou (China) that from 2000 to 2013, the land surface temperature increased with the increase of the proportion of development land, and the proportion of green space decreased sharply. In addition, this study also quantified RLST changes in BA and DE's eco-land use returns less than BA and DE's loss during urbanization (2000-2020) and regional urban development. This result shows the value and importance of the existing natural ecological system, because the newly built 'ecological' land does not provide the same cooling effect. Moreover, the existing grasslands still play an important role in mitigating RTE due to the larger RLST changes caused by the conversion of grassland to development land than the conversion of development land to grassland. Therefore, these strategies can focus on how to improve the cooling performance of the current grassland through better adaptive management and planning (i.e., establishing tree-shrub-grass structure).

4.3 Limitations and further research

It is necessary to point out some limitations of this study. Firstly, in this study, we have not considered the corresponding temperature from the meteorological service database for comparison and verification. If ground measurement can be used in future research, it may be better. Second, the mechanism and reasons for the difference in the cooling effect of ecological land gains and losses still need further study. In addition, analyses such as climate change, anthropogenic heat emissions and the coupling effects of urban agglomerations need further study. Combined with the indicators of human social and economic activities, the driving mechanism of the spatial and temporal evolution characteristics of the blue-green space cooling island in the EJRLLZ was explored and analyzed. In addition, in order to alleviate the intensification of urban agglomeration heat island diffusion, the 'green ecological group' is constructed in the cities of the EJRLLZ, and the 'green ecological barrier' is established between cities. As an important carrier of the ventilation corridor, the blue-green space focuses on the simulation of the scene model of the ventilation corridor in the central urban area and the oxygen source green space in the urban fringe area. Through the cooling islands such as 'green corridor' and 'blue road (Haihe River and Lake) ', the ventilation network is formed to guide the flow of the wind in various regions of the city to prevent the spread of the high temperature area of the heat island. Therefore, in the future, it is necessary to gradually realize the fine simulation of different scales through the nested coupling of mesoscale numerical model and small scale numerical model. Multi-scale numerical simulation technology can be composed of regional scale (100-200 km), urban scale (10-20 km) and block scale (1-2 km). WRF, MMS, RBLM and other mesoscale meteorological models can be used for regional scale simulation, and CFD softwares such as Fluent, Phoenics, ENVI-met can be used for urban and block scale simulation.

5. Conclusion

This study examines one of the regions that have been greatly affected by the urbanization of world-class urban agglomerations in the past 20 years (EJRLLZ), and examines the impact of urbanization and urban agglomeration development (2000-2020) on regional blue-green space and RTE pattern and evolution. The study found that from 2000 to 2020, the development land increased significantly and the arable land decreased significantly in the EJRLLZ. Isolated urban heat island (UHI) is gradually connected and interacted, especially in Chuzhou, Yangzhou and Taizhou. There is a trend of forming regional heat island (RHI), while regional cooling island is gradually fragmented. We suggest that the blue-green space is not only dominated by specific land cover types, but also significantly affected by specific land conversion processes.

In particular, we also reveal that there is a significant difference between the cooling effect of ecological land loss and income, which indicates that the existing ecological land (especially water and wetland) is very valuable for climate adaptation, because the newly constructed ecological land does not have the same effect on cooling effect. In theory, this study demonstrates the impact of land cover transfer process on the blue-green space in the period of urbanization, improves the understanding of the dynamics of blue-green space in rapid urbanization (especially urban agglomeration development), and provides important insights for the protection of existing natural ecosystems and climate adaptation planning.

Author Contributions: For research articles with several authors, a short paragraph specifying their individual contributions must be provided. The following statements should be used "Conceptualization, F.Q. and Z.P.; methodology, J.Z.; software, Z.L.; validation, J.Z. formal analysis, Z.L.; investigation, F.Q.; resources, F.Q.; data curation, Z.P.; writing—original draft preparation, Z.P.; writing—review and editing, F.Q.; All authors have read and agreed to the published version of the manuscript.", please turn to the CRediT taxonomy for the term explanation. Authorship must be limited to those who have contributed substantially to the work reported.

Funding: The research work was financially supported by the National Science & Technology Infrastructure of China (No. 2005DKA32300), the Major Projects of the Ministry of Education (No. 16JJD770019), the Data Sharing Infrastructure of Earth System Science Data Centre of the Lower Yellow River Region (http://henu.geodata.cn) and Geospatial Data Cloud site, the attribution Climatic Research Unit, University of East Anglia, and the Asian Precipitation - Highly-Resolved Observational Data Integration Towards Evaluation (APHRODITE), Computer Network Information Center, Chinese Academy of Sciences (http://www.gscloud.cn).

Conflicts of Interest: The authors declare no conflict of interest.

Reference

1. IPCC. Climate change 2007: The physical science basis. Working group icontribution to the fourth assessment report of the intergovernmental panel onclimate change. *Cambridge, UK: Cambridge University Press.* **2007**.
2. Kong, F.; Yin, H.; James, P.; Hutyra, L.R.; He, H.S. Effects of spatial pattern of greenspace on urban cooling in a large metropolitan area of eastern china. *Landscape and Urban Planning* **2014**, *128*, 35-47.
3. Jia, W.; Zhao, S. Trends and drivers of land surface temperature along the urban-rural gradients in the largest urban agglomeration of china. *Sci Total Environ* **2020**, *711*, 134579.
4. Fang, C. Important progress and future direction of studies on china's urban agglomerations. *Journal of Geographical Sciences* **2015**, *25*, 1003-1024.
5. Wu, J.; Yang, S.; Zhang, X. Interaction analysis of urban blue-green space and built-up area based on coupling model—a case study of wuhan central city. *Water* **2020**, *12*.
6. Wenguang, Z.; Wenjuan, W.; Guanglei, H.; Chao, G.; Ming, J.; Xianguo, L. Cooling effects of different wetlands in semi-arid rural region of northeast china. *Theoretical and Applied Climatology* **2020**, *141*, 31-41.

7. Wang, Y.; Zhan, Q.; Ouyang, W. How to quantify the relationship between spatial distribution of urban waterbodies and land surface temperature? *Sci Total Environ* **2019**, *671*, 1-9.
8. Dong, Z.D.Z.L.Z.L.F.H.L. The effect of landscape park on urban heat island: A case study of harbin city. *AREAL RESEARCH AND DEVELOPMENT* **2011**, *30*, 73-78.
9. Sun, R.; Chen, A.; Chen, L.; Lü, Y. Cooling effects of wetlands in an urban region: The case of beijing. *Ecological Indicators* **2012**, *20*, 57-64.
10. Adams L W, D.L.E. Wildlife reserves and corridors in the urban environment: Aguide to ecological landscape planning and resource conservation[m]. *National Institute for Urban Wildlife, Columbia* **1989**, *MD*.
11. Cao, X.; Onishi, A.; Chen, J.; Imura, H. Quantifying the cool island intensity of urban parks using aster and ikonos data. *Landscape and Urban Planning* **2010**, *96*, 224-231.
12. Yu, Z.; Yang, G.; Zuo, S.; Jørgensen, G.; Koga, M.; Vejre, H. Critical review on the cooling effect of urban blue-green space: A threshold-size perspective. *Urban Forestry & Urban Greening* **2020**, *49*.
13. Yu, Z.; Fryd, O.; Sun, R.; Jørgensen, G.; Yang, G.; Özdil, N.C.; Vejre, H. Where and how to cool? An idealized urban thermal security pattern model. *Landscape Ecology* **2020**.
14. Yang, G.; Yu, Z.; Jørgensen, G.; Vejre, H. How can urban blue-green space be planned for climate adaption in high-latitude cities? A seasonal perspective. *Sustainable Cities and Society* **2020**, *53*.
15. Zhou, D.; Bonafoni, S.; Zhang, L.; Wang, R. Remote sensing of the urban heat island effect in a highly populated urban agglomeration area in east china. *Sci Total Environ* **2018**, *628-629*, 415-429.
16. Wu, J. Urban ecology and sustainability: The state-of-the-science and future directions. *Landscape and Urban Planning* **2014**, *125*, 209-221.
17. Jun, C.; Ban, Y.; Li, S. Open access to earth land-cover map. *Nature* **2014**, *514*, 434-434.
18. CHENG Chen, C.Z., YAN Wei, HAO Cui, LI Hong-yuan, MO Xun-qiang. Study of temporal and spatial variation of urban heat island based on landsat tm in central city and binhai new area of tianji. *JOURNAL OF NATURAL RESOURCES* **2010**, *25*.
19. Ranhao; Sun; Liding; Chen. Effects of green space dynamics on urban heat islands: Mitigation and diversification. *Ecosystem Services* **2017**, *23*, 38-46.
20. Zou, Z.; Qiu, G.Y.; Li, X.; Li, H.; Guo, Q.; Yan, C.; Tan, S. Experimental studies on the effects of green space and evapotranspiration on urban heat island in a subtropical megacity in china. *AGUFM* **2016**, *2016*.
21. Takada, T.; Miyamoto, A.; Hasegawa, S.F. Derivation of a yearly transition probability matrix for land-use dynamics and its applications. *Landscape Ecology* **2010**, *25*, 561-572.
22. Yu, Z.; Yao, Y.; Yang, G.; Wang, X.; Vejre, H. Strong contribution of rapid urbanization and urban agglomeration development to regional thermal

environment dynamics and evolution. *Forest Ecology and Management* **2019**, *446*, 214-225.
23. Santamouris, M. Cooling the cities – a review of reflective and green roof mitigation technologies to fight heat island and improve comfort in urban environments. *Solar Energy* **2014**, *103*, 682-703.
24. Santarnouris, M.; Kolokotsa, D. On the impact of urban overheating and extreme climatic conditions on housing, energy, comfort and environmental quality of vulnerable population in europe. *Energy & Buildings* **2015**, *98*, 125-133.
25. Peng, J.; Xie, P.; Liu, Y.; Jing, M. Urban thermal environment dynamics and associated landscape pattern factors: A case study in the beijing metropolitan region. *Remote Sensing of Environment* **2016**, *173*, 145-155.
26. Du, H.; Cai, Y.; Zhou, F.; Jiang, H.; Jiang, W.; Xu, Y. Urban blue-green space planning based on thermal environment simulation: A case study of shanghai, china. *Ecological Indicators* **2019**, *106*.
27. Wang, Z.; Liu, M.; Liu, X.; Meng, Y.; Zhu, L.; Rong, Y. Spatio-temporal evolution of surface urban heat islands in the chang-zhu-tan urban agglomeration. *Physics and Chemistry of the Earth, Parts A/B/C* **2020**, *117*.
28. Masoudi, M.; Tan, P.Y.; Liew, S.C. Multi-city comparison of the relationships between spatial pattern and cooling effect of urban green spaces in four major asian cities. *Ecological Indicators* **2019**, *98*, 200-213.
29. Srivanit, M.; Hokao, K. Evaluating the cooling effects of greening for improving the outdoor thermal environment at an institutional campus in the summer. *Building and Environment* **2013**, *66*, 158-172.
30. Onishi, A.; Cao, X.; Ito, T.; Shi, F.; Imura, H. Evaluating the potential for urban heat-island mitigation by greening parking lots. *Urban Forestry & Urban Greening* **2010**, *9*, 323-332.
31. Ng, E.; Chen, L.; Wang, Y.; Yuan, C. A study on the cooling effects of greening in a high-density city: An experience from hong kong. *Building and Environment* **2012**, *47*, 256-271.
32. Lobaccaro, G.; Acero, J.A. Comparative analysis of green actions to improve outdoor thermal comfort inside typical urban street canyons. *Urban Climate* **2015**, *14*, 251-267.
33. Lee, H.; Mayer, H.; Chen, L. Contribution of trees and grasslands to the mitigation of human heat stress in a residential district of freiburg, southwest germany. *Landscape and Urban Planning* **2016**, *148*, 37-50.
34. Lee, D.; Oh, K.; Seo, J. An analysis of urban cooling island (uci) effects by water spaces applying uci indices. *International Journal of Environmental Science and Development* **2016**, *7*, 810-815.
35. Gonçalves, A.; Ornellas, G.; Castro Ribeiro, A.; Maia, F.; Rocha, A.; Feliciano, M. Urban cold and heat island in the city of bragança (portugal). *Climate* **2018**, *6*.
36. Du, H.; Song, X.; Jiang, H.; Kan, Z.; Wang, Z.; Cai, Y. Research on the cooling island effects of water body: A case study of shanghai, china. *Ecological Indicators* **2016**, *67*, 31-38.

37. Du, H.; Cai, W.; Xu, Y.; Wang, Z.; Wang, Y.; Cai, Y. Quantifying the cool island effects of urban green spaces using remote sensing data. *Urban Forestry & Urban Greening* **2017**, *27*, 24-31.
38. Suchul; Kang; Elfatih, A.B.; Eltahir. North china plain threatened by deadly heatwaves due to climate change and irrigation. *Nature communications* **2018**.
39. Cheng, L.; Guan, D.; Zhou, L.; Zhao, Z.; Zhou, J. Urban cooling island effect of main river on a landscape scale in chongqing, china. *Sustainable Cities and Society* **2019**, *47*.
40. Chen, A.; Yao, L.; Sun, R.; Chen, L. How many metrics are required to identify the effects of the landscape pattern on land surface temperature? *Ecological Indicators* **2014**, *45*, 424-433.
41. Chang, C.-R.; Li, M.-H.; Chang, S.-D. A preliminary study on the local cool-island intensity of taipei city parks. *Landscape and Urban Planning* **2007**, *80*, 386-395.
42. Zhaowu; Guo; Xieying; Zeng; Yuxi; Koga; Motoya; Vejre; Henrik. Variations in land surface temperature and cooling efficiency of green space in rapid urbanization: The case of fuzhou city, china. *Urban Forestry & Urban Greening* **2018**.